

Contents lists available at ScienceDirect

Radiotherapy and Oncology

journal homepage: www.thegreenjournal.com



Original Article

3D printed 2D range modulators preserve radiation quality on a microdosimetric scale in proton and carbon ion beams



Sandra Barna ^{a,*}, Cynthia Meouchi ^b, Andreas Franz Resch ^a, Giulio Magrin ^c, Dietmar Georg ^{a,c}, Hugo Palmans ^{c,d}

^a Department of Radiation Oncology, Medical University of Vienna, Waehringer Guertel 18-20; ^b Atominstitut, Technical University of Vienna, Stadionallee 2, Vienna; ^c MedAustron Ion Therapy Center, Marie-Curie-Straße 5, Wiener Neustadt, Austria; ^d National Physical Laboratory, Hampton Road, Teddington, United Kingdom

ARTICLE INFO

Article history: Received 27 November 2022 Received in revised form 31 January 2023 Accepted 1 February 2023 Available online 11 February 2023

Keywords:
Particle therapy
2D range modulator
2D ripple filter
Microdosimetry
Monte Carlo simulation

ABSTRACT

Introduction: Particle therapy using pencil beam scanning (PBS) faces large uncertainties related to ranges and target motion. One possibility to improve existing mitigation strategies is a 2D range modulator (2DRM). A 2DRM offers faster irradiation times by reducing the number of layers and spots needed to create a spread-out Bragg peak. We have investigated the impact of 2DRM on microdosimetric spectra measured in proton and carbon ion beams.

Materials and Methods: Two 2DRMs were designed and 3D printed, one for.

124.7 MeV protons and one for 238.6 MeV/u carbon ions. Their dosimetric validation was performed using Roos and PinPoint ionization chamber and EBT3 films. Monte Carlo simulations were done using GATE. A silicon-based solid-state microdosimeter was used to collect pulse-height spectra along three depths for two irradiation modalities, PBS and a single central beam.

Results: For both particle types, the original pin design had to be optimized via GATE simulations. The difference between the R80 of the simulated and measured depth dose curve was 0.1 mm. The microdosimetric spectra collected with the two irradiation modalities overlap well. Their mean lineal energy values differ over all positions by 5.2 % for the proton 2DRM and 2.1 % for the carbon ion 2DRM.

Conclusion: Radiation quality in terms of lineal energy was independent of the irradiation method. This supports the current approach in reference dosimetry, where the residual range is chosen as a beam quality index to select stopping power ratios.

© 2023 The Author(s). Published by Elsevier B.V. Radiotherapy and Oncology 182 (2023) 109525 This is an open access article under the CC BY license (http://creativecommons.org/licenses/by/4.0/).

Introduction

Particle therapy is known for its unique ability to create dose distributions for complex structures with high conformity using active scanning [1–3]. However, this precision comes with the price of increased uncertainties on ranges (due to using CT images and stopping power databases for treatment planning) and target motion. The latter can be caused by inter- or intrafractional motion, with the biggest concern being respiratory motion [4]. Several mitigation techniques are in use to counter this, like abdominal compression, gating, rescanning, or 4D robust optimization [5]. During the last years, an efficient delivery technique was proposed and could be used to improve mitigation strategies, e.g. in combination with breath-hold techniques: 2D and 3D range modulators (2DRM, 3DRM), which are best described as a 3D printed filter, sometimes in combination with a range shifter [6]. 2DRMs have

old review paper by Chu et al. [7], a similar filter is described. These are called "ridge filters" and several designs are discussed, e.g., static bar ridge filters or rotating spiral ridge filters. With an advance in Monte Carlo (MC) techniques and 3D printing, the new ridge filter generation is becoming more accessible for many different applications. The 2DRM and 3DRM publications from recent years use a single-energy beam that is uniformly delivered over the whole filter. The shape of the 2DRM/3DRM causes an appropriate

a universal pin design and are suitable for cell studies or preclinical experiments. For more complex applications like the conformal irradiation of a tumor, 3DRMs are better with their non-

homogenous pin designs. For both types, other terms have been

used such as 2D ridge filter or 2D pin filter for the 2DRM, and 3D

desired dose distribution is not new. In an almost two decades

The concept of passively scattering particle beams to create a

conformal range modulator or hedgehog filter for the 3DRM.

in a spread-out Bragg peak (SOBP).

A 2DRM eliminates the need for using different energies to create a SOBP, instead it modulates a single energy into a SOBP with

mixing of particles with different transmitted energies, resulting

^{*} Corresponding author at: Medizinische Universitate Wien, Universitätsklinik für Radioonkologie, Waehringer Guertel 18-20, 1090 Wien, Austria. E-mail address: sandra.barna@meduniwien.ac.at (S. Barna).

its unique pin design. This allows for faster irradiation times while still resulting in a dose distribution comparable to the energy-modulated SOBP approach. Dynamic 2DRMs and 3DRMs offer benefits for patients [8,9], which are faster treatment plans and less interplay effect due to hot and cold spots. 2DRMs have versatile areas of application, for example in radiobiological studies [10] they help to reduce the time spent outside of the incubator, therefore the stress on the cells is reduced. Another application is in FLASH radiotherapy, where experiments have been carried out with a 2DRM [11,30]. Disadvantages of 2DRMs are their dependence on the particle type, energy and target position. Better dose conformity is also achieved with pencil beam scanning (PBS) instead of passively scattered beams, due to lower range straggling and lower lateral diffusion.

If a 2DRM is used for cell irradiations, it is possible to perform additional measurements at the corresponding depths in water with microdosimetric detectors. The collected spectra in lineal energy can be used for the prediction of relative biological effectiveness (RBE) based on the average values of the probability density distributions in frequency and in dose, y_F and y_D . The most prevalent radiobiological model based on microdosimetric spectra is the microdosimetric kinetic model (MKM) [12,13], which was proposed by Hawkins in 1996. Since then, the model has served as a basis for further developments, for example the modified MKM [14,15] or the Mayo Clinic Florida MKM [16].

Ideally, the collection of microdosimetric spectra and the cell irradiation for cell survival curves studies occur under the same experimental conditions. The sensitive volume (SV) of microdosimeters is naturally quite small (in the order of a few μm) while the field size of radiobiological SOBP plans is usually larger (in the order of a few cm). A single pencil beam, broadened by a 2DRM, is enough to cover the entire SV of a microdosimeter and is a time-efficient option. But whether such a single central spot (CS) would result in the same radiation quality as a large volume irradiation delivered with PBS needs to be demonstrated.

In principle, the modification through overlapping neighbouring beams (during PBS) was expected to have an impact on the lowest part of the microdosimetric spectra. This is due to a higher amount of delta rays produced inside of the detector crossing air gaps as well as contributions from fragments from neighbouring spots. Using a solid-state detector, microdosimetric spectra were collected with both irradiation modes (CS and PBS) for protons and carbon ions. According to dosimetry protocols, such as TRS-398 [17], CS and PBS are the same in terms of beam quality specifications. We investigated this in terms of microdosimetry and showed that the use of 3D printed 2DRMs for microdosimetric research is feasible and especially useful in combination with cell survival studies.

Materials and methods

Design of 2DRM

For protons and carbon ions, a pin design (see Fig. 1) was optimized following the approach suggested by Simeonov et al. [6]. The pins are placed side-by-side over a base plate with a chosen thickness. GATE/Geant4 simulations were performed to create a dose distribution look-up table with varying scattering materials 5 cm downstream the nozzle exit window for a single energy (50 steps with 1 mm resolution in water equivalent thickness (WET)). The details of the GATE/Geant4 beam model can be found in previous studies [18,19]. The optimization algorithm was implemented in Matlab R2020a. The script minimized the sum of the squared differences between the desired and current dose distribution, which was calculated by multiplying a weighting vector with the tabulated dose matrix. A side objective (sigmoidal function) was added

to the cost function to prevent negative and low weights. The weights resulting from this optimization were then converted to pin base and height values and exported as Standard Template Library files (stl) for 3D printing.

The initial goal was to create a SOBP with a 4 cm modulation length and a range of 10 cm in accordance with the standard setting for treatment plans for biological research at our institute. Based on the range, the nominal beam energies were chosen as 124.7 MeV for the proton beam and 238.6 MeV/u for the carbon ion beam. The finished designs were printed using a 3D stereolithography (SLA) printer by Formlabs with an XY resolution of 25 μm .

Both filters were printed using a synthetic resin, a material named by Formlabs as white resin. Its relative water-equivalent thickness (rWET) was measured to be 1.18. This was relevant for the material definition in the MC simulations. Since no chemical composition was given by the manufacturer, the chemical composition of PMMA was used with a reduced density of 1.16 g cm⁻³, which resulted in the desired rWET = 1.18.

After the dosimetric verification (see II B) the pin design was reoptimized for better agreement with the measured depth doses (Roos chamber measurements at different lateral positions). This so-called virtual pin design (see Fig. 1) will be used for future MC simulations of spectra in lineal energy.

Dosimetric verification

For each particle type, both 2DRMs were validated using two different types of ionization chambers (IC) as well as gafchromic films (EBT3, Ashland, New Jersey, USA). For both IC measurements, a temperature and pressure correction was performed. The treatment plan had a field size of 17 cm \times 9 cm.

First, depth doses at different lateral positions were acquired with the 0.35 cc Roos® Electron Chamber (PTW, Freiburg, Germany) in a motorized water phantom (MP3-P, PTW, Freiburg, Germany). Twenty-four PTW-31015 PinPoint chambers were used in combination with a 3D detector block holder, placed at six depths, four ICs in a row. Details about this set- up can be found elsewhere [20,21]. PinPoint measurements were performed at five depths along the SOBP (44.1 mm, 57.3 mm, 76.0 mm, 93.7 mm, 96.5 mm). For each depth six lateral positions were selected, horizontally (X) and vertically (Y) shifted from the isocenter by X/Y = (±1.5 cm, 0.0 cm/±4 cm, 0.0 cm).

EBT3 films were cut to 5 cm \times 5 cm pieces. A stack of three films was placed at five depths along the depth dose curve, and for each depth at the isocenter (0 cm) as well as at two lateral positions (\pm 5 cm). This way the majority of the treatment plan could be checked for local non-uniformities. The EBT3 films were scanned 48 h post irradiation in transmission mode with an EPSON Expression 11000XL scanner (Seiko Epson Corporation, Nagano, Japan), and non-irradiated films were used to subtract the background. To exclude any artefacts from cutting or markings for positioning, a circle with a radius of 3 cm was defined as a region of interest. Scanned images were converted to absorbed dose to water applying a previously established calibration curve for proton and carbon ion beams [22].

The homogeneity of the EBT3 films was assessed using the homogeneity index HI, which was calculated using the formula D_5/D_{95} , with D_5 and D_{95} being the minimum dose to 5 % and 95 % of the target voxels. Ideally, the HI would be one and it increases with less homogeneous dose distributions [23].

Microdosimetric verification

A silicon-based detector, developed at the University of Wollongong [24], was used for the microdosimetric measurements. This so-called 3D mushroom detector consists of an array of 400 SVs, each

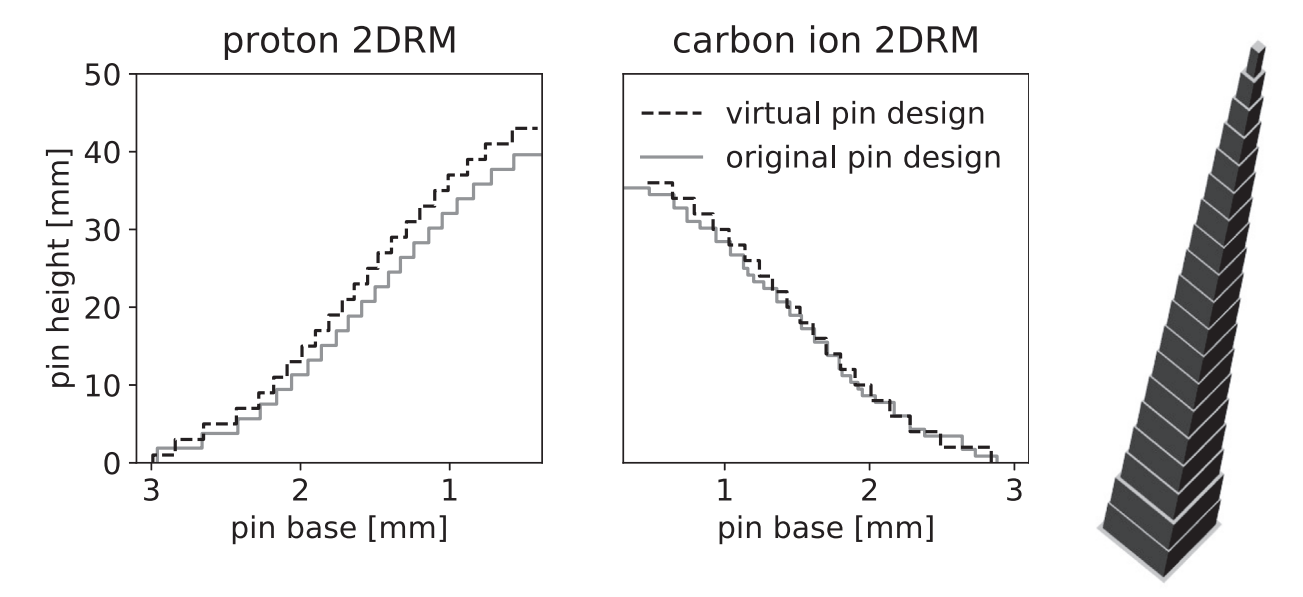


Fig. 1. The original versus virtual pin design for the two 2DRMs. For both beam types, the pin height was increased and the pin bases remained similar.

with a diameter of 18 μ m placed on a high resistivity p-type silicon on insulator active layer with a 10 μ m thickness [25]. The 3D mush-room detector, as well as a low noise pre- and shaping amplifier constituted the MicroPlus probe. All pulses were collected with a multichannel analyzer (ORTEC 928 MCB), which transforms the analog shaping amplifier output into a digital signal and displays the pulse-height spectrum. The frequency and shape of the pulses were monitored with an oscilloscope. Some pile-up events were recorded.

The MicroPlus probe with the 400 SVs was placed along the central axis inside a stationary water phantom (Water Phantom 41,023 for Horizontal Beams, PTW Freiburg, Germany) with the help of an in-house developed holder. The 2DRM was set up 40 cm upstream the water phantom's entrance window. Measurements at the same position were recorded consecutively without entering the irradiation room, guaranteeing no changes in depth between the pulseheight spectra acquisition of the two irradiation modes.

For both protons and carbon ions, we collected six spectra at three depths along the central axis. For each depth, either a treatment plan of dimensions 2 cm \times 2 cm was delivered with PBS, or a beam with a single central spot was loaded. For the proton/carbon

ion treatment plan, the FWHM of the spots (at isocenter with $80\,\%$ degrader) was $11.8\,$ mm/ $7.0\,$ mm and the spot spacing was $3\,$ mm/ $2\,$ mm, respectively.

The multi-channel analyzer output was processed with an inhouse developed Excel file. Detailed information about the different steps of calculating microdosimetric spectra, e.g. the linearization of the electronic chain or the calibration via the proton edge technique, can be found elsewhere [26].

Results

(Optimized) design of 2DRM

Fig. 2 shows two different MC simulation results for the proton and carbon ion 2DRM compared to the dosimetric measurements with the Roos IC. For the proton 2DRM, the original filter design shows a shift of 1.9 mm at R80 (range at 80 % dose) between the two data sets. Based on the Roos data, a new base plate thickness of (8.5 mm instead of 5.7 mm) was chosen and the pin design was optimized to fit the measurements. This resulted in excellent

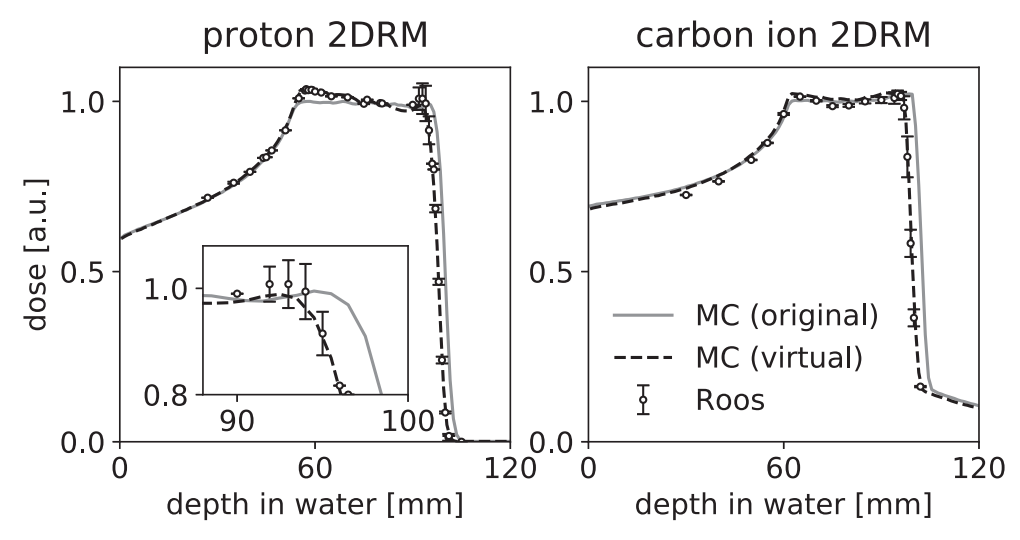


Fig. 2. The results of the MC simulation with the original and virtual pin design for protons (left) and carbon ions (right) in comparison with the Roos measurements.

agreement (Δ R80 = 0.1 mm) between the measured and simulated depth dose curve. On average, the pin base was changed by 0.1 mm while the pin height was changed by 0.2 mm. This changed pin design, solely used for the purpose of MC simulations, is referred to as virtual pin design throughout this manuscript.

The same optimization process was repeated for the carbon ion 2DRM (the base plate thickness was 8.5 mm instead of 6 mm). While the number of individual stacks was increased by only one for the proton 2DRM, they were decreased by 32 % for the carbon ion 2DRM, therefore a direct comparison of changes in pin base and height is idle. An improvement of the shift at R80 between the measured and simulated depth dose curve was achieved with $\Delta R80 = 0.4$ mm instead of $\Delta R80 = 3.2$ mm.

Dosimetric verification

For the proton/carbon ion 2DRM Roos measurements, the mean over the relative standard deviations of all measurement points in the fall-off region below R90 was 2.0 %/7.6 %, which translates to a depth uncertainty of 0.1 mm/0.3 mm. The reciprocal of the depth dose gradient at R80 was used as a sensitivity coefficient. The uncertainty from type B errors for this set-up was estimated to be 0.2 mm elsewhere [27]. This results in an overall positioning uncertainty of 0.2 mm for the proton 2DRM and 0.4 mm for the carbon ion 2DRM.

For the 24 PinPoint set-up, the mean and standard deviation of each PinPoint IC for each depth was calculated over the seven off-axis positions, resulting in 120 values. Therefore, the results are given as a range for the low gradient (plateau and SOBP) and high gradient (fall-off) regions. In the proton beam, the relative standard deviations of the low gradient regions were up to 1.8 %, while the

high gradient region showed higher fluctuations resulting in a relative standard deviation between 0.4 % and 4.4 %. For the carbon ion 2DRM, the relative standard deviations were up to 0.9 % for the low gradient regions and between 0.4 % and 2.0 % for the high gradient region.

The HI was assessed for each film individually. The mean HI over each stack of films can be found in Table 1. The mean of means over all five positions was 1.17 for the proton 2DRM and 1.14 for the carbon ion 2DRM.

Microdosimetric verification

Fig. 3 shows all measured spectra in lineal energy, using the dose probability distribution representation [28]. Excellent agreement was observed between the two different irradiation modalities, PBS versus a single CS. The differences in the cut-off values (0.65 keV/ μ m for the proton 2DRM and up to 5 keV/ μ m for the carbon ion 2DRM) are explained by different amplifications (medium and low gain) during the measurements.

The mean lineal energies in frequency y_F and in dose y_D , calculated on the linearly binned spectra above the noise threshold, are shown in Table 2. Overall, the agreement between the mean lineal energy values of PBS and CS is between 1 % and 6 %. The only outlier is the plateau position for the proton 2DRM, where deviations go up to 14 % for the dose mean lineal energy.

Discussion

The results of the three different dosimetric techniques (Roos, 24 PinPoints, EBT3 films) are consistent with each other. The deviations found between the planned and measured R80 position can

Table 1 Homogeneity index HI = D_5/D_{95} for both particle types.

depth along SOBP	HI of proton 2DRM			HI of carbon 2DRM		
	+ 5 cm	0 cm	−5 cm	+ 5 cm	0 cm	−5 cm
plateau near 80 % dose	1.10 ± 0.01	1.11 ± 0.03	1.11 ± 0.02	1.08 ± 0.00	1.09 ± 0.02	1.09 ± 0.00
begin of SOBP	1.13 ± 0.04	1.11 ± 0.03	1.13 ± 0.01	1.08 ± 0.00	1.09 ± 0.00	1.08 ± 0.00
middle of SOBP	1.12 ± 0.02	1.11 ± 0.01	1.10 ± 0.01	1.10 ± 0.00	1.10 ± 0.02	1.09 ± 0.01
end of SOBP	1.13 ± 0.02	1.16 ± 0.04	1.16 ± 0.05	1.15 ± 0.02	1.11 ± 0.02	1.12 ± 0.01
fall-off near 80 % dose	1.30 ± 0.10	1.43 ± 0.10	1.28 ± 0.12	1.36 ± 0.05	1.32 ± 0.01	1.20 ± 0.01

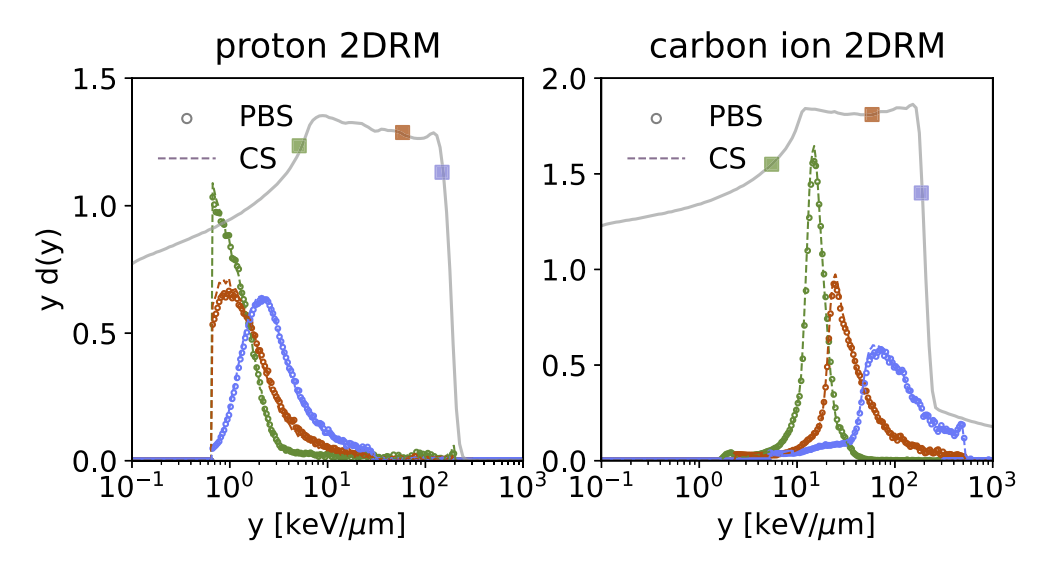


Fig. 3. Dose distribution of the lineal energy for both particle types at different depths along the SOBP. The scattered data points represent the spectra measured with PBS, while the dashed lines represent the spectra measured with a single CS. The x-axis is mirrored to show the position along the SOBP where the spectra were collected.

Table 2
Mean lineal energy in frequency \bar{y}_F and in dose \bar{y}_D . Values are given for both irradiation modalities, pencil beam scanning (PBS) and central spot (CS). The differences Δ between the two modalities are given in percent.

depth in water	$\bar{y}_{F,PBS}$ [ke V $\mu \mathrm{m}^{\text{-1}}$	$\bar{y}_{F,\mathrm{CS}}$ [ke V $\mu\mathrm{m}^{\text{-1}}$	$\Delta [\%]$	$\bar{y}_{D,PBS}$ [ke V $\mu \mathrm{m}^{-1}$	$\bar{y}_{D,\mathrm{CS}}$ [ke V $\mu\mathrm{m}^{-1}$	Δ [%]
proton 2DRM						
52.2 mm	1.11	1.10	0.9 %	3.70	4.22	13.9 %
83.0 mm	1.38	1.31	4.5 %	3.10	3.02	2.7 %
95.1 mm	2.26	2.20	2.9 %	4.13	3.87	6.2 %
carbon ion 2DRM						
52.2 mm	12.77	12.89	1.0 %	16.43	16.34	0.6 %
83.0 mm	24.07	24.67	2.5 %	50.14	50.68	1.1 %
98.1 mm	55.44	58.94	6.3 %	124.10	122.90	1.0 %

be explained by a thicker base plate while the slightly different SOBP width is most likely caused by slight differences in the pin bases. Also, the end of the SOBP showed a high variability based on the off-axis positioning of the Roos chamber (up to 6 cm), which is expressed as a high uncertainty of the mean Roos and PinPoint measurements over all depth dose measurements. This might indicate that the 3D SLA printer by Formlabs is not suitable for such filigree work. Based on these findings, we recommend a thorough investigation of the off-axis depth dose of 3D printed 2DRMs before any cell samples are placed in a potential high uncertainty region.

The differences between the MC simulated dose and the measured dose were overcome by the optimization of the pin design. Whether this optimization corrected only uncertainties in the 3D printing process or also in any physics computations, e.g., a lack of scattering modelled by Geant4, could not be derived from our data

When using a different type of microdosimeter, i.e., a tissue-equivalent proportional counter (TEPC), a 2DRM could also be beneficial. TEPCs can only be operated with low particle rates (flux). If the flux is reduced by a few orders of magnitude, the dose delivery system might not be able to measure the position of the particle beam anymore and therefore the feedback mechanism to the scanning magnets will not be operational for PBS. In our institute, this means that low fluxes are only available with a monoenergetic single spot, delivered at the isocenter. Even in these cases, spectra along a SOBP could be collected with TEPCs if a 2DRM is used.

TRS-398 [17] uses the residual range as a beam quality specifier regardless of initial beam energy or delivery method (scanned vs scattered). Our findings support this claim for modulated beams regarding the independence of delivery method used, i.e., that the residual range as a beam quality specifier represents the radiation quality with sufficient uniqueness for dosimetry purposes, regardless of the range of the beam.

The expected influence on the microdosimetric spectra by an increase in delta rays when the 2DRM is irradiated with PBS rather than a CS was not seen in our measurements with a solid-state microdosimeter. This would have been especially visible in the mean lineal energy in frequency, y_F , as this quantity is influenced most by delta rays. Solid state microdosimeters have a moderate low energy sensitivity [29], leading to higher cut-off values that could mask any delta ray effects. Further measurements using a more sensitive microdosimeter, i.e., a TEPC, should be carried out. This way, any effects down to 0.3 keV/ μ m can be investigated.

In the past, plan libraries with molds for collimators were used in conventional radiotherapy. For PBS in proton or carbon ion therapy, a 2DRM offers the possibility to advance this idea and create a plan library basis with a multitude of SOBP widths and ranges. This would be especially useful for cell and animal experiments.

A more dynamic solution to the rigid design of the 2DRM was suggested by Maradia et al [8]. They propose the use of two identical 2DRM, which are placed in front of the isocenter. Their rela-

tive position to each other causes a broadening of the Bragg peak. This way different dose distributions can be achieved with the same 2DRMs, by matching peaks to peaks (maximum Bragg peak broadening) or matching peaks to valleys (no broadening), and everything in between.

Another advantage of using 2DRM is in the area of FLASH, especially in combination with animal experiments. Singers Sørensen et al. [30] irradiated the right hind limb of 301 mice with a monoenergetic proton beam with conventional and FLASH dose rates. A 2DRM can create a mixed energy field (and therefore a SOBP) that cannot be created by PBS for FLASH dose rates. In combination with a collimator, more precise treatments could be delivered. This way, tumor instead of limb irradiations with FLASH dose rates would be possible.

The next step will be to create a treatment plan matching the range and SOBP width of the measured 2DRM dose distributions. This treatment plan will be delivered using active PBS with no passive beam modifier, and microdosimetric measurements will be repeated. This way, a complete analysis comparing active PBS, passive PBS and a passive CS on a microdosimetric scale will be completed.

Conclusion

The specification of the radiation quality in terms of lineal energy is independent of the irradiation method in passively scattered beams. This has meaning beyond the 2DRM application. In reference dosimetry, the residual range is used as a selection parameter for the stopping power ratios of monoenergetic beams. A constant radiation quality in terms of lineal energy regardless of irradiation modality (at the same position along the Bragg peak) underlines the validity of this approach.

Declaration of Competing Interest

The authors declare that they have no known competing financial interests or personal relationships that could have appeared to influence the work reported in this paper.

Acknowledgements

This work was supported by the Austrian Science Fund (FWF) through project number P32103-B. The authors have no conflicts to disclose.

References

- [1] Chang JY, Zhang X, Knopf A, Li H, Mori S, Dong L, et al. Consensus guidelines for implementing pencil-beam scanning proton therapy for thoracic malignancies on behalf of the ptcog thoracic and lymphoma subcommittee. Int J Radiat Oncol Biol Phys 2017;99:41.
- [2] Apinorasethkul O, Kirk M, Teo K, Swisher-McClure S, Lukens JN, Lin A. Pencil beam scanning proton therapy vs rotational arc radiation therapy: a treatment

- planning comparison for postoperative oropharyngeal cancer. Med Dosim 2017:42:7.
- [3] J. in Kim, J. M. Park, and H.-G. Wu, Carbon ion therapy: A review of an advanced technology, Progress in Medical Physic 31, 71 (2020)
- [4] Mori S, Zenklusen S, Inaniwa T, Furukawa T, Imada H, Shirai T, et al. Conformity and robustness of gated rescanned carbon ion pencil beam scanning of liver tumors at nirs. Radiother Oncol 2014;111:431.
- [5] Engwall E, Fredriksson A, Glimelius L. 4d robust optimization including uncertainties in time structures can reduce the interplay effect in proton pencil beam scanning radiation therapy. Med Phys 2018;45:4020.
- [6] Simeonov Y, Weber U, Penchev P, Ringbæk TP, Schuy C, Brons S, et al. 3D range-modulator for scanned particle therapy: development, monte carlo simulations and experimental evaluation. Phys Med Biol 2017;62:7075.
- [7] Chu WT, Ludewigt BA, Renner TR. Instrumentation for treatment of cancer using proton and light-ion beams. Rev Sci Instrum 1993;64:2055.
- [8] Maradia V, Colizzi I, Meer D, Weber DC, Lomax AJ, Actis O, et al. Universal and dynamic ridge filter for pencil beam scanning particle therapy: a novel concept for ultra-fast treatment delivery. Phys Med Biol 2022;67:225005.
- [9] Ringbæk TP, Weber U, Santiago A, Iancu G, Wittig A, Grzanka L, et al. Validation of new 2D ripple filters in proton treatments of spherical geometries and non-small cell lung carcinoma cases. Phys Med Biol 2018;63:245020.
- [10] Simeonov Y, Weber U, Schuy C, Engenhart-Cabillic R, Penchev P, Durante M, et al. Monte carlo simulations and dose measurements of 2D rangemodulators for scanned particle therapy. Z Med Phys 2021;31:203.
- [11] Tessonnier T, Mein S, Walsh DW, Schuhmacher N, Liew H, Cee R, et al. Flash dose rate helium ion beams: first in vitro investigations. Int J Radiat Oncol Biol Phys 2021;111:1011.
- [12] Hawkins RB. A microdosimetric-kinetic model of cell death from exposure to ionizing ra- diation of any LET, with experimental and clinical applications. Int J Radiat Biol 1996;69:739.
- [13] Hawkins RB. A microdosimetric-kinetic theory of the dependence of the RBE for cell death on LET. Med Phys 1998;25:1157.
- [14] Kase Y, Yamashita W, Matsufuji N, Takada K, Sakae T, Furusawa Y, et al. Microdosimetric calculation of relative biological effectiveness for design of therapeutic proton beams. J Radiat Res 2013;54:485.
- [15] Chen Y, Li J, Li C, Qiu R, Wu Z. A modified microdosimetric kinetic model for relative biological effectiveness calculation. Phys Med Biol 2017;63.
- [16] Parisi A, Beltran C, Furutani K. The mayo clinic florida microdosimetric kinetic model of clonogenic survival: formalism and first benchmark against in vitro and in silico data. Phys Med Biol 2022. accepted for publication.

- [17] IAEA, Technical Report Series No. 398: Absorbed Dose Determination in External Beam Radiotherapy, Tech. Rep. (IAEA, 2000)
- [18] Resch AF, Elia A, Fuchs H, Carlino A, Palmans H, Stock M, et al. Evaluation of electromagnetic and nuclear scattering models in gate/geant4 for proton therapy. Med Phys 2019;46:2444.
- [19] Elia A, Resch AF, Carlino A, Böhlen TT, Fuchs H, Palmans H, Letellier V, Dreindl R, Osorio J, Stock M, Sarrut D, Grevillot L. A gate/geant4 beam model for the medaustron non-isocentric proton treatment plans quality assurance. Phys Med 2020;71:115.
- [20] Karger CP, Jakel O, Hartmann GH, Heeg P. A system for three-dimensional dosimetric verification of treatment plans in intensity-modulated radiotherapy with heavy ions. Med Phys 1999;26:2125.
- [21] Carlino A, Stock M, Zagler N, Marrale M, Osorio J, Vatnitsky S, et al. Characterization of PTW-31015 PinPoint ionization chambers in photon and proton beams. Phys Med Biol 2018;63:185020.
- [22] Grevillot L, Stock M, Palmans H, Moreno JO, Letellier V, Dreindl R, et al. Implementation of dosimetry equipment and phantoms at the medaustron light ion beam therapy facility. Med Phys 2018;45:352.
- [23] V. A. Semenenko, B. Reitz, E. Day, X. S. Qi, M. M. M, and X. A. Li, Evaluation of a commercial biologically based imrt treatment planning system, Med Phys 35, 5851 (2008)
- [24] Tran LT, Prokopovich DA, Petasecca M, Lerch MLF, Kok A, Summanwar A, et al. 3D radiation detectors: Charge col- lection characterisation and applicability of technology for microdosimetry. IEEE Trans Nucl Sci 2014;61:1537.
- [25] Tran LT, Chartier L, Prokopovich DA, Bolst D, Povoli M, Summanwar A, et al. Thin silicon microdosimeter utilizing 3-d mems fabrication technology: charge collection study and its application in mixed radiation fields. IEEE Trans Nucl Sci 2018;65:467.
- [26] Meouchi C, Barna S, Puchalska M, Tran LT, Rosenfeld A, Verona C, et al. On the measurement uncertainty of microdosimetric quantities using diamond and silicon microdosimeters in carbon-ion beams. Med Phys 2022. accepted for publication.
- [27] Barna S, Resch AF, Puchalska M, Georg D, Palmans H. Technical note: experimental determination of the effective point of measurement of the ptw-31010 ionization chamber in proton and carbon ion beams. Med Phys 2022:49:675
- [28] ICRU, ICRU REPORT 36: Microdosimetry, Tech. Rep. (AAPM, 1983)
- [29] Bradley PD, Rosenfeld AB, Zaider M. Solid state microdosimetry. Nucl Instrum Methods Phys Res, Sect B 2001;184:135.
- [30] Sørensen BS, Sitarz MK, Ankjærgaard C, Johansen J, Andersen CE, Kanouta E, et al. In vivo validation and tissue sparing factor for acute damage of pencil beam scanning proton flash. Radiother Oncol 2022;167:109.